J|A|C|S
ARTICLES
Published on Web 02/19/2005

Lanthanide Clusters with Internal Ln Ions: Highly Emissive Molecules with Solid-State Cores

Anna Kornienko,[†] Thomas J. Emge,[†] G. Ajith Kumar,[‡] Richard E. Riman,[‡] and John G. Brennan*,[†]

Contribution from the Department of Chemistry and Chemical Biology and Department of Materials Engineering, Rutgers, the State University of New Jersey, 610 Taylor Road, Piscataway, New Jersey 08854-8087

Received October 19, 2004; E-mail: bren@ccbmail.rutgers.edu

Abstract: "$Er(SePh)_{2.5}I_{0.5}$" reacts with elemental S to give $(THF)_{10}Er_6S_6I_6$, a double cubane cluster with one face of the Er_4S_4 cube capped by an additional Er_2S_2. Reactions with a mixture of elemental S/Se results in the formation of $(THF)_{14}Er_{10}S_6(Se_2)_6I_6$, a cluster composed of an Er_6S_6 double cubane core, with two "$Er_2(Se_2)_3$" units condensed onto opposing rectangular sides of the Er_6S_6 fragment. This deposition of Er_2Se_6 totally encapsulates the two central Er with chalcogen atoms (4 S, 4 Se) and excludes neutral THF donors or iodides from the two primary coordination spheres. The Er_{10} compound is the first lanthanide cluster to contain internal, chalcogen encapsulated Ln. This cluster shows strong fluorescence at 1544 nm with a measured decay time of 3 ms and an estimated quantum efficiency of 78%, which is comparable to Er doped solid-state materials. The unusual fluorescence spectral properties of $(THF)_{14}Er_{10}S_6Se_{12}I_6$ are unprecedented for a molecular Er complex and are attributed to the low phonon energy host environment provided by the I^-, S^{2-}, and Se_2^{2-} ligands.

Introduction

Extraordinary developments in transition metal cluster chemistry have provided considerable insight into the size-dependent physical properties of quantum-confined systems.[1−5] Synthetic studies with these covalent metals (M = Zn, Cd, Hg, Cu, Ag....) have produced extremely large metal chalcogenido (E, E = S, Se, Te) cluster compounds with precisely defined cluster surfaces and internal, chalcogenido-encapsulated M.[6−8] Most of these internal M have coordination environments that resemble the environments found in bulk solid-state materials. With both molecular and solid-state characteristics, these clusters represent a unique opportunity to develop novel materials with superior physical properties.

The analogous cluster chemistry of the lanthanides (Ln) is considerably less developed.[9−20] Ionic Ln form comparatively unstable (i.e., heat, water, oxygen, and light sensitive) compounds with S, Se, and Te, and these experimental complications tend to inhibit progress within the field. One particularly general synthetic approach to Ln clusters with chalcogenido anions involves reduction of elemental E by the chalcogenolates ligands in $Ln(EPh)_3$.[9−17]

Common to all isolable LnE_x clusters is the coordination of at least one ancillary ligand to each Ln in a compound, a feature that contrasts dramatically with abundance of internal, chalcogen encapsulated M. In most LnE_x compounds, these ancillary ligands are neutral Lewis bases (i.e., THF, pyridine, DME) and or X^- (X = EPh, I). Similarly, in the limited series of organometallic lanthanide chalcogen cluster compounds,[18,19] every Ln coordinates to a relatively electronegative Cp ligand. The tendency of Ln to avoid encapsulation by these electropositive E ligands is consistent with the view of these metals as oxophilic, but even with oxo ligands,[21−25] Ln cluster

[†] Department of Chemistry and Chemical Biology.
[‡] Department of Materials Engineering.

(1) Steckel, J. S.; Zimmer, J. P.; Coe-Sullivan, S.; Stott, N. E.; Bulovic, V.; Bawendi, M. G. *Angew. Chem., Int. Ed.* **2004**, *43*, 2154−2158.
(2) Kim, S.; Lim, Y. T.; Soltesz, E. G.; De Grand, A. M.; Lee, J.; Nakayama, A.; Parker, J. A.; Mihaljevic, T.; Laurence, R. G.; Dor, D. M.; Cohn, L. H.; Bawendi, M. G.; Frangioni, J. V. *Nat. Biotechnol.* **2004**, *22*, 93−97.
(3) Steckel, J. S.; Coe-Sullivan, S.; Bulovic, V.; Bawendi, M. G. *Adv. Mater.* **2003**, *15*, 1862−1866.
(4) Liu, J.; Tanaka, T.; Sivula, K.; Alivisatos, A. P.; Frechet, J. M. *J. Am. Chem. Soc.* **2004**, *126*, 6550−6551.
(5) Yin, Y.; Rioux, R. M.; Erdonmez, C. K.; Hughes, S.; Somorjai, G. A.; Alivisatos, A. P. *Science* **2004**, *304*, 711−714.
(6) Degroot, M. W.; Corrigan, J. F. *Comput. Coord. Chem. II* **2004**, *7*, 57−123.
(7) Ahlrichs, R.; Eichhoefer, A.; Fenske, D.; Hampe, O.; Kappes, M. M.; Nava, P.; Olkowska-Oetzel, J. *Angew. Chem., Int. Ed.* **2004**, *43*, 3823−3827.
(8) Fenske, D.; Persau, C.; Dehnen, S.; Anson, C. E. *Angew. Chem., Int. Ed.* **2004**, *43*, 305−309.
(9) Freedman, D.; Emge, T. J.; Brennan, J. G. *J. Am. Chem. Soc.* **1997**, *119*, 11112.
(10) Melman, J. H.; Emge, T. J.; Brennan, J. G. *Chem. Commun.* **1997**, 2269.
(11) Melman, J. H.; Emge, T. J.; Brennan, J. G. *Inorg. Chem.* **1999**, *38*, 2117.
(12) Freedman, D.; Emge, T. J.; Brennan, J. G. *Inorg. Chem.* **1999**, *38*, 4400.
(13) Freedman, D.; Melman, J. H.; Emge, T. J.; Brennan, J. G. *Inorg. Chem.* **1998**, *37*, 4162.
(14) Fitzgerald, M.; Emge, T. J.; Brennan, J. G. *Inorg. Chem.* **2002**, *41*, 3528.
(15) Freedman, D.; Emge, T. J.; Brennan, J. G. *Inorg. Chem.* **2002**, *41*, 492.
(16) Kornienko, A.; Emge, T. J.; Hall, G.; Brennan, J. G. *Inorg. Chem.* **2002**, *41*, 121.
(17) Kornienko, A.; Emge, T. J.; Brennan, J. G. *J. Am. Chem. Soc.* **2001**, *123*, 11933.
(18) Evans, W. J.; Rabe, G. W.; Ansari, M. A.; Ziller, J. W. *Angew. Chem., Int. Ed. Engl.* **1994**, *33*, 2110.
(19) Cheng, Y.; Jin, G. X.; Shen, Q.; Lin, Y. *J. Organomet. Chem.* **2001**, *94*, 631.
(20) Cary, D. R.; Ball, G. E.; Arnold, J. *J. Am. Chem. Soc.* **1995**, *117*, 3492.
(21) Westin, G.; Moustiakimov, M.; Kritikos, M. *Inorg. Chem.* **2002**, *41*, 3249−3258.
(22) Giester, G.; Unfried, P.; Zak, Z. *J. Alloys Compd.* **1997**, *257*, 175−181.
(23) Deng, D.; Zhang, Y.; Dai, C.; Zeng, H.; Ye, C.; Hage, R. *Inorg. Chim. Acta* **2000**, *310*, 51−55.

chemistry has yet to reach the level of achievement set by main group and transition metal chemists.

As one of the most interesting fundamental goals of cluster chemistry is to study the evolution of physical properties along the pathway connecting molecules, clusters, and solid-state compounds, it is important to be able to prepare increasingly larger cluster compounds with both surface and internal Ln. Such products are expected to exhibit unprecedented chemical or physical properties, optimally incorporating the key advantages of molecular and solid-state materials.

In the lanthanide domain, one ideal combination of molecular and solid-state physical properties would unite the emission properties of solid-state Ln materials with the solubility properties of molecular compounds. Er(III) has an emission at 1.54 μm that has extensive applications in optical fiber signal amplification.[26−30] While this emission has been studied extensively in solid-state materials (e.g., halides, chalcogenides, and oxides), the ability to stimulate emission from molecular Er sources has been hampered by the accompanying high phonon energies of hydrocarbon- or hydroxide-based coordination spheres, which can easily bridge the energy transitions desired for erbium and thus nonradiatively quench emission.[31−6] Thus, the short lifetimes and low intensities of these compounds have lessened interest in these molecular complexes. Soluble, molecular compounds with a coordination environment similar to those provided by solid-state materials could be useful for delivering emissive Er ions into less conventional matrixes.

Outlined here is a heterochalcogen approach to the synthesis of increasingly large cluster compounds. Using a lanthanide sulfido cluster as a nucleation site, $Ln_2(Se_2)_3$ fragments are attached to the sides of the sulfido core, generating a larger cluster with internal, chalcogen encapsulated lanthanide ions. The emission properties of this material are compared with related molecular and solid-state materials.

Experimental Section

General Methods. All syntheses were carried out under ultrapure nitrogen (JWS), using conventional drybox or Schlenk techniques. Solvents (Fisher) were refluxed continuously over molten alkali metals or K/benzophenone and were collected immediately prior to use. Anhydrous pyridine (Aldrich) was purchased and refluxed over KOH. Er was purchased from Strem. PhSeSePh was purchased from Aldrich and recrystallized from hexane. Melting points were taken in sealed capillaries and are uncorrected. IR spectra were taken on a Mattus Cygnus 100 FTIR spectrometer and recorded from 4000 to 600 cm^{-1} as a Nujol mull on NaCl plates. Electronic spectra were recorded on a Perkin-Elmer (Lambda 9) spectrometer with the samples in a 0.10 mm quartz cell attached to a Teflon stopcock. Elemental analyses were performed by Quantitative Technologies, Inc. (Whitehouse NJ).

Synthesis of $(THF)_{10}Er_6S_6I_6$·6 THF (1): Er (335 mg, 2.0 mmol), PhSeSePh (624 mg, 2.0 mmol), iodine (269 mg, 1.0 mmol), and Hg (50 mg, 0.25 mmol) were combined in THF (50 mL). The mixture was stirred until all the metal was consumed. To the resultant pink solution elemental S (64 mg, 2.0 mmol) was added. After 24 h the yellow solution was filtered and layered with hexanes (15 mL) to give pink crystals (0.29 g, 32%) that do not melt but turn gray at 274 °C. Anal. Calcd for $C_{64}H_{128}O_{18}Er_6I_6S_6$: C, 24.7; H, 4.15. Found: C, 24.4; H, 3.81. UV−vis (4-ethylpyridine): 550 (ϵ = 0.45), 522 (ϵ = 1.1) nm. IR: 3170 (s), 2905 (w), 2723 (s), 2680 (s), 2359 (s), 2342 (s), 2214 (s), 1959 (s), 1869 (s), 1602 (s), 1575 (s), 1456(w), 1377 (m), 1367 (m), 1306 (s), 1260 (s), 1220 (m), 1176 (m), 1071 (w), 1038 (m), 1006 (w), 950 (s), 913 (m), 846 (w), 734 (s), 669 (s) cm^{-1}.

Synthesis of $(THF)_{14}Er_{10}S_6(Se_2)_6I_6$·3 THF (2): Er (330 mg, 2 mmol), PhSeSePh (749 mg, 2.4 mmol), iodine (153 mg, 0.6 mmol), and Hg (50 mg, 0.25 mmol) were combined in THF (60 mL). The mixture was stirred until all the metal was consumed to give a pink solution. Elemental Se (190 mg, 2.4 mmol) was added, and the reaction mixture was stirred for 2 h. After that, elemental S (36 mg, 1.2 mmol) was added. After a day, the orange solution (50 mL) was filtered, layered with hexanes (15 mL), and completely covered with aluminum foil. In a week, yellow crystals (0.30 g, 31%) appeared which do not melt but turn dark brown at 249 °C. Anal. Calcd for $C_{68}H_{136}O_{17}I_6S_6Se_{12}Er_{10}$: C, 17.0; H, 2.86. Found: C, 17.2; H, 2.39. The compound is insoluble in THF and does not show an optical absorption maximum from 300 to 800 nm in pyridine. IR: 3169 (s), 2943 (w), 2727 (s), 2675 (s), 1636 (s), 1461(w), 1377 (w), 1306 (s), 1261 (s), 1169 (s), 1074 (m), 1037 (s), 1008 (m), 915 (m), 857 (m), 722 (m) cm^{-1}.

X-ray Structure Determination of 1 and 2. Data for **1** and **2** were collected on a Bruker Smart APEX CCD diffractometer with graphite monochromatized Mo Kα radiation (λ = 0.710 73 Å) at 100 K. The data were corrected for Lorenz effects, polarization, and absorption, the latter by a multiscan (SADABS)[37] method. The structures were solved by Patterson methods (SHELXS86).[38] All non-hydrogen atoms were refined (SHELXL97)[39] based upon F_{obs}^2. All hydrogen atom coordinates were calculated with idealized geometries (SHELXL97). Scattering factors (f_o, f', f'') are as described in SHELXL97. Crystallographic data and final R indices for **1** and **2** are given in Table 1. ORTEP diagrams[40] for **1** and **2** are shown in Figures 1 and 2, respectively, while color representations of the core atoms for **1** and **2** are given in Figure 3. Significant bond geometries for **1** and **2** are given in the figure captions. Complete crystallographic details for **1** and **2** are given in the Supporting Information.

Optical Properties. The infrared emission spectra were recorded by exciting the sample with a 980 nm band of a laser diode in the 45° excitation geometry. Emission from the sample was focused onto a 1 m monochromator (Jobin Yvon, Triax 550, Edison, NJ) and detected by a thermoelectrically cooled InGaAs detector (EO Systems, Phoenixville, PA). The signal was intensified with a lock-in amplifier (Stanford Research System, SR 850 DSP, Sunnyvale, CA) and processed by computer using Spectramax software (GRAMS 32, Salem, NH). The

(24) Kritikos, M.; Moustiakimov, M.; Wijk, M.; Westin, G. *J. Chem. Soc., Dalton Trans.* **2001**, 1931−1938.
(25) Wang, R.; Carducci, M. D.; Zheng, Z. *Inorg. Chem.* **2000**, *39*, 1836−1837.
(26) Becker, P. C.; Olsson, N. A.; Simpson, J. R. *Erbium doped fiber amplifiers-Fundamental and technology*; Academic Press: NY, 1999.
(27) Fick, J.; Knystautas. E. J.; Villeneuve, A.; Schiettekatte, A.; Roorda, S.; Richardson, K. A, *J. Non-Cryst. Solids* **2000**, *272*, 200.
(28) Ye, C. C.; Hewak, D. W.; Hempstead, M.; Samson, M.; Payne, D. N, *J. Non-Cryst. Solids* **1996**, *208*, 56.
(29) Washburn, B. R.; Diddams, S. A.; Newbury, N. R.; Nicholson, J. W.; Yan, M. F.; Jorgensen, C. G. *Optics Lett.* **2004**, *29*, 250−252.
(30) Yiannopoulos, K.; Vyrsokinos, K.; Tsiokos, D.; Kehayas, E.; Pleros, N.; Theophilopoulos, G.; Houbavlis, T.; Guekos, G.; Avramopoulos, H. *IEEE J. Quantum Elect.* **2004**, *40*, 157−165.
(31) Hebbink, G. A.; Reinboudt, D. N.; van Veggel, F. C. J. M *Eur. J. Org. Chem.* **2001**, 4101.
(32) Sloof, L. H.; Polman, A. *J. Appl. Phys* **1998**, *83*, 497.
(33) Wolbers, M. P. O.; van Veggel, F. C. J. M.; Snellink-Ruel, B. H. M.; Hofstraat, J. W.; Geurts, F. A. J.; Reinhoudt. D. N. *J. Am. Chem. Soc.* **1997**, *119*, 138.
(34) Wolbers, M. P. O.; van Veggel, F. C. J. M.; Peters, F. G. A.; van Beelen, E. S. E.; Hofstraat, J. W.; Geurts, F. A. J.; Reinhoudt, D. N. *Chem.—Eur. J.* **1998**, *4*, 772.
(35) Hasegawa, Y.; Okhubo, T.; Sogabe, K.; Kawamura, Y.; Wada, Y.; Nakashima, N.; Yanagida, S. *Angew. Chem., Int. Ed.* **2000**, *39*, 357.
(36) Kumar, G A.; Ballato, J.; Snitzer, E.; Riman, R *J. Appl. Phys*, **2004**, *95*, 40.
(37) Bruker-ASX. *SADABS, Bruker Nonius area detector scaling and absorption correction*, v2.05; Bruker-AXS Inc.: Madison, Wisconsin, 2003.
(38) Sheldrick, G. M. *SHELXS86, Program for the Solution of Crystal Structures*; University of Göttingen: Germany, 1986.
(39) Sheldrick, G. M. *SHELXL97, Program for Crystal Structure Refinement*; University of Göttingen: Germany, 1997.
(40) (a) Johnson, C. K. ORTEP II, Report ORNL-5138. Oak Ridge National Laboratory, Oak Ridge, TN, 1976. (b) Zsolnai, L. *XPMA and ZORTEP, Programs for Interactive ORTEP Drawings*; University of Heidelberg: Germany, 1997.

Table 1. Summary of Crystallographic Details for **1** and **2**

compound	**1**	**2**
empirical formula	$C_{64}H_{128}Er_6I_6O_{16}S_6$	$C_{68}H_{136}Er_{10}I_6O_{17}S_6Se_{12}$
fw	3110.98	4799.65
space group	$P\bar{1}$	$C2/c$
a (Å)	12.3560(8)	27.688(6)
b (Å)	13.8550(9)	18.146(4)
c (Å)	14.4095(9)	23.794(5)
α(deg)	92.114(1)	90.00
β(deg)	106.369(1)	106.390(4)
γ (deg)	99.122(1)	90.00
V (Å^3)	2328.2(3)	11 469(4)
Z	1	4
D(calcd) (g/cm^{-3})	2.219	2.780
temp (K)	100(2)	100(2)
λ (Å)	0.710 73	0.710 73
abs coeff (mm^{-1})	7.521	12.810
$R(F)^a$ [$I > 2\sigma(I)$]	0.0390	0.0615
$R_w(F^2)^a$ [$I > 2\sigma(I)$]	0.0927	0.1274

[a] Definitions: $R(F) = \Sigma||F_o| - |F_c||/\Sigma|F_o|$; $R_w(F^2) = \{\Sigma[w(F_o^2 - F_c^2)^2]/\Sigma[w(F_o^2)^2]\}^{1/2}$. Additional crystallographic details are given in the Supporting Information.

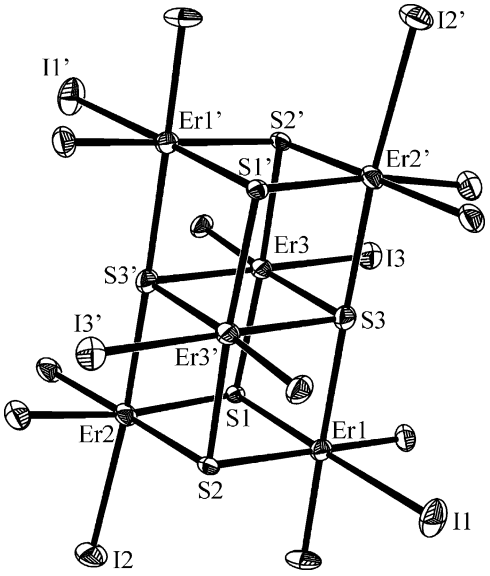

Figure 1. ORTEP diagram of the double cubane cluster $(THF)_{10}Er_6S_6I_6$ with thermal ellipsoids are drawn at the 50% probability level, the oxygen atoms unlabeled, and the C and H atoms removed for clarity. Significant distances (Å) and angles (deg) for **1**: Er(1)−O(1), 2.329(4); Er(1)−S(2), 2.6671(15); Er(1)−S(1), 2.6777(15); Er(1)−S(3), 2.7292(15); Er(1)−S(3)′, 2.7793(14); Er(1)−I(2), 3.0027(5); Er(2)−O(3), 2.327(4); Er(2)−O(2), 2.335(4); Er(2)−S(2)′, 2.6383(15); Er(2)−S(1), 2.6656(15); Er(2)−S(3), 2.6907(14); Er(2)−I(3), 3.0237(5); Er(3)−O(4), 2.338(4); Er(3)−O(5), 2.368(4); Er(3)−S(2), 2.6505(15); Er(3)−S(1)′, 2.6530(14); Er(3)−S(3), 2.7006(14); Er(3)−I(1), 2.9836(5).

luminescence lifetime of the infrared emission was measured by the same laser modulated by a mechanical chopper, and the signals were collected by a digital oscilloscope (HP 54520A, 500 MHz, Hewlett-Packard Instruments, Santa Clara, CA).

Results

The sulfido cluster $(THF)_{10}Er_6S_6I_6$ (**1**) is isolated from the reaction of "ErI(SePh)$_2$" with elemental S in THF at room temperature (reaction 1). The compound exhibits the characteristic light pink color of Er(III) and is soluble in THF or pyridine. Structural analysis of this compound reveals a double cubane framework,[13,16] with one face of an Er_4S_4 cubane cluster capped by an additional Er_2S_2 layer. Figure 1 shows an ORTEP diagram of **1**, and the figure caption gives a listing of significant

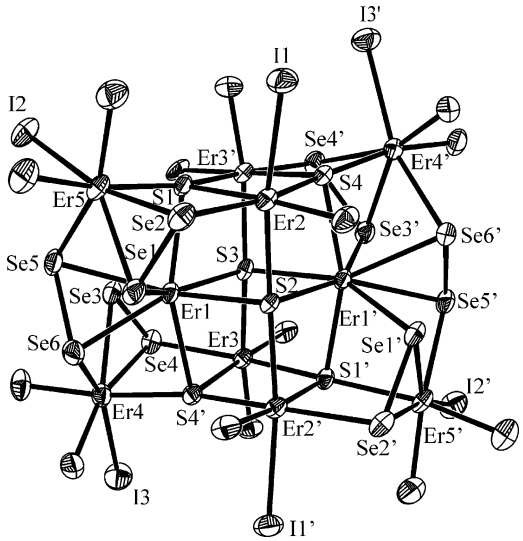

Figure 2. Molecular structure of the decanuclear heterochalcogen cluster **2** with the thermal ellipsoids drawn at the 50% probability level, the oxygen atoms unlabeled, and the C and H atoms removed for clarity. Significant distances (Å) for **2**: Er(1)−S(1), 2.781(4); Er(1)−S(4)′, 2.814(4); Er(1)−S(2), 2.834(4); Er(1)−S(3), 2.866(4); Er(1)−Se(6), 2.907(2); Er(1)−Se(3), 2.933(2); Er(1)−Se(1), 3.013(2); Er(1)−Se(5), 3.0471(19); Er(2)−O(1), 2.333(13); Er(2)−S(4), 2.662(5); Er(2)−S(2), 2.6770(10); Er(2)−S(1), 2.723(5); Er(2)−Se(2), 2.823(2); Er(2)−I(1), 2.9986(15); Er(3)−O(2), 2.294(12); Er(3)−O(3), 2.301(11); Er(3)−S(3), 2.5944(12); Er(3)−S(1)′, 2.664(5); Er(3)−S(4)′, 2.676(5); Er(3)−Se(4), 2.833(2); Er(4)−O(5), 2.344-(13); Er(4)−O(4), 2.343(14); Er(4)−S(4)′, 2.676(5); Er(4)−Se(3), 2.785-(2); Er(4)−Se(4), 2.887(2); Er(4)−Se(6), 2.961(2); Er(4)−I(3), 3.0375(16); Er(5)−O(6), 2.300(14); Er(5)−O(7), 2.359(13); Er(5)−S(1), 2.671(4);Er-(5)−Se(1), 2.769(2); Er(5)−Se(2), 2.903(2); Er(5)−Se(5), 2.906(2); Er-(5)−I(2), 3.0451(18). Symmetry transformations used to generate equivalent atoms: $-x + 1, y, -z + 1/2$.

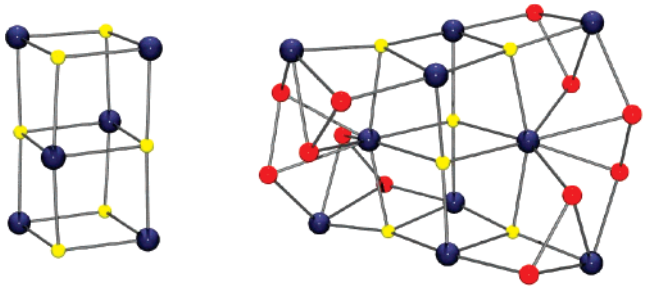

Figure 3. Core structures of $(THF)_{10}Er_6S_6I_6$ (left) and $(THF)_{14}Er_{10}S_6(Se_2)_6I_6$ (right), with blue Er, yellow S, and red Se. The THF and I ligands have been removed for clarity.

bond lengths and angles for the compound. There are single terminal iodides coordinated to all six Er, and the remaining octahedral coordination sites are saturated with THF ligands. Geometries about the Ln are nearly octahedral, and Er−S bond lengths appear to have a directional dependence,[13,16] with Er−S bonds trans to I consistently longer than related bonds trans to the O atoms of THF, for both μ_3-S and μ_4-S ligands.

$$\mathrm{Er} + \mathrm{PhSeSePh} + 0.5\ \mathrm{I_2} \xrightarrow{\mathrm{THF}} \text{“ErI(SPh)}_2\text{”} \xrightarrow{\mathrm{S}} (\mathrm{THF})_{10}\mathrm{Er_6S_6I_6} + \mathrm{PhSeSePh} \quad (1)$$

Increasing the starting ratio of Ln/I and adding a mixture of S/Se results in the formation of $(THF)_{14}Er_{10}S_6(Se_2)_6I_6$ (reaction 2). A low-temperature single-crystal X-ray diffraction analysis of **2** was obtained, and an ORTEP diagram for **2** is given in Figure 2, with significant bond lengths and angles given in the

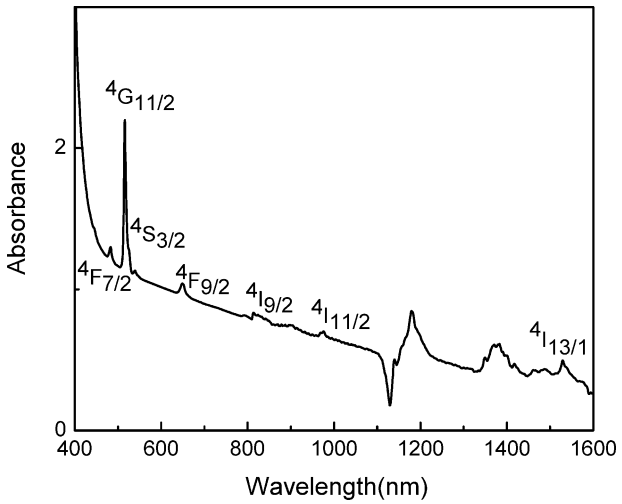

Figure 4. Absorption spectrum of $(THF)_{14}Er_{10}S_6Se_{12}I_6$ with standard assignments for the various spectral transitions.

figure caption. In **2**, the central Er_6S_6 core has been capped on two opposite sides by $Er_2(Se_2)_3$ units that displace the I and THF coordinated to the two inner Er and encapsulating them entirely by chalcogenido (4 S, 4 Se) ligands (Figure 3).

$$10\ Er + 12\ Ph_2Se_2 + 3\ I_2 \xrightarrow{THF} \text{“}ErI_{0.6}(SePh)_{2.4}\text{”} \xrightarrow{S,\ Se} (THF)_{10}Er_{10}S_6Se_{12}I_6 + 12\ Ph_2Se_2 \quad (2)$$

Significant structural perturbations appear within the Er_6S_6 framework upon coordination of the two $Er_2(Se_2)_3$ units. At the central Er, the four coordinating S are all displaced to one side to accommodate the change in coordination number from six to eight. The average Ln−S−Ln and S−Ln−S angles along the length of the Er_6S_6 cube are now 169.6° and 160.3°, respectively, in contrast with the analogous structural parameters in octahedral sites of **1** (177° and 171°). This increased coordination number also results in a significant lengthening of all the central Er−S bond lengths. These six S are now all μ_4 donors, and their bond length range (0.06 Å), while still significant, is now half of the 0.11 Å range in Ln−S bond lengths found in **1**.

Cluster **2** is yellow because of a localized electronic excitation on the diselenide ligand[41] that masks the characteristic Er color. Representative absorption and emission spectra of **2** are shown in Figures 4 and 5, respectively. The emission spectrum of Er-doped LaF_3 nanocrystals having comparable Er concentration is shown for comparative purposes.[42] The pump photons at 980 nm populate the $^4I_{11/2}$ excited state. A part of the excited population decays to $^4I_{13/2}$ by multiphonon relaxation, and the remaining population will appear as radiative decay by the $^4I_{13/2} \rightarrow {}^4I_{15/2}$ channel, which is responsible for the 1542 nm emission. The lifetime of this emission was extracted from an exponential curve fit of the 1542 nm fluorescence decay (see Supporting Information) with a value of 3 ms. With this fluorescence decay time the quantum yield of 1542 nm emission can be estimated from the ratio of the fluorescence decay time (τ_{fl}) to radiative or “natural” decay time (τ_r). With a calculated radiative decay time of 3.85 ms following the Judd−Ofelt

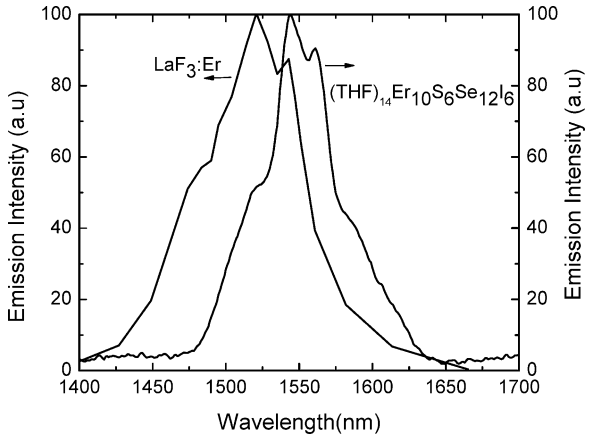

Figure 5. Comparison of the emission spectrum of Er^{3+} in $(THF)_{14}Er_{10}S_6Se_{12}I_6$ (8.71×10^{20} ions/cc, fwhm 61 nm, stimulated emission cross section 4.1×10^{-21} cm^2, quantum efficiency 78%) and Er-doped LaF_3 nanocrystals (22.6×10^{20} ions/cc, fwhm 73 nm, stimulated emission cross section 3.3×10^{-21} cm^2, quantum efficiency 100%).

Table 2. Comparison of the Fluorescence Spectral Data of Infrared Emission in $(THF)_{10}Er_6S_6I_6$ and LaF_3/Er

properties	$(THF)_{10}Er_6S_6I_6$	LaF_3:Er
radiative decay time (τ_{rad}, ms)	3.85	12.3
fluorescence decay time (τ_{fl}, ms)	3	12.3
qunatum efficiency (%)	78	100
emission cross section (σ_e, cm^2)	4.1×10^{-21}	3.3×10^{-21}
emission bandwidth ($\Delta\lambda$, nm)	61	73
ionic concentration (ions/cm^3)	8.71×10^{20}	22.6×10^{20}

procedure[43,44] a quantum efficiency of 78% is obtained for **2**. Both decay time and quantum efficiency values represent averages for all Er in the cluster. The fluorescence spectral width (fwhm) and stimulated emission cross-section are estimated to be, respectively, 61 nm and 4.1×10^{-21} cm^2, which are comparable to the well-known host LaF_3/Er (Table 2).[42] With 61 and 1542 nm, an available optical bandwidth of 7.5 THz is obtained.

Discussion

Compound **2** represents the first example of a lanthanide cluster that contains Ln ions appropriately described as “internal”, rather than “surface” Ln. This differentiation is important because an evaluation of size-dependent physical properties depends on our ability to deliver a series of increasingly large clusters. This “heterochalcogen” approach, by which more nucleophilic chalcogens are buried with the cluster core and less nucleophilic chalcogens “cap” the cluster surface, is a potentially general approach to the synthesis of both larger clusters and ternary solid-state materials. When this approach is coupled with the recent observation that EE ligands in Ln-$(EE)_x$ clusters can be reduced to E^{2-} with $Ln(EPh)_3$,[17] the stage is then set for the stepwise synthesis of increasingly larger molecules.

Until the present example, isolable lanthanide clusters with core, chalcogenido encapsulated Ln were unknown. In molecular work, an all-sulfur coordination sphere has been noted once in $Yb(SBu^t)_6^{3-}$,[45] but subsequent investigations[46] have always

(41) Schlaich, H.; Lindner, G.-G.; Feldmann, J.; Göbel, E. O.; Reinen, D. *Inorg. Chem.* **2000**, *39*, 2740.
(42) Kumar, G A.; Ballato, J.; Snitzer, E.; Riman, R *J. Appl. Phys*, **2004**, *95*, 40.
(43) Judd, B. R. *Phys. Rev. B: Condens. Matter* **1962**, *127*, 750.
(44) Ofelt, G. S. *J. Chem. Phys.* **1962**, *37*, 511.
(45) Cetinkaya, B.; Hitchcock, P. B.; Lappert, M. F.; Smith, R. G. *J. Chem. Soc., Chem. Commun.* **1992**, 932.
(46) Nief, F. *Coord. Chem. Rev.* **1998**, *178−180*, 13.

produced compounds with at least one more electronegative donor atom included within the primary Ln coordination sphere. Of the chalcogenido clusters in the literature, only the base free tellurolate decomposition product[20] $Ce_5Te_3(TeSi(SiMe_3)_3)_9$ has been described, and the transient nature of this product unfortunately precluded detailed characterization. In all the isolable chalcogenido clusters, every Ln has been bound to at least one THF, DME, or pyridine ligand.

Cluster **2** also contains S^{2-} ligands that can be described as internal, rather than surface atoms. Chalcogen "encapsulation" by Ln is also uncommon but has been noted in the structure of $(DME)_7Nd_7S_7(SePh)_6^+$,[9] which contained a single μ_5-sulfido ligand in a tetragonal pyramidal geometry. Organometallic clusters have also contained Ln encapsulated Se^{2-}, in both $Cp^*_6Sm_6Se_{11}$[18] and the ionic clusters[19] $[Na(THF)_6]_2[Cp^t_6Sm_6Se_{13}]$ and $[Li(THF)_4]_2[Cp_6Nd_6Se_{13}]$, where central μ_6Se^{2-} ligands are enveloped by an octahedral array of Ln(III), an environment found in solid-state LnE (NaCl).[47−49]

With internal E^{2-} and Ln, **2** can be compared with solid-state LnE_x materials. Geometries about the internal S^{2-} in **2** are not as ideal as the internal octahedral E^{2-} in the organometallic derivatives, and they also have lower coordination numbers than S^{2-} ions in solids, i.e., Tm_2S_3,[50,51] where the five-coordinate S have Tm−S−Tm angles that resemble a tetragonal pyramid. Similarly, the two eight-coordinate encapsulated Er-(1) have the highest CN in the cluster; yet these are still not as high as the CN in the monocapped square antiprisms found in the structure of Ho_8S_{15}.[52] It is worth noting that, in contrast, geometries about both S and M in the group 12 MS clusters are all ideal tetrahedra,[6] just as they are in binary solid-state MS compounds.

The chalcogen atoms in **2** are surprisingly ordered. Random arrays of S and Se in heterochalcogen materials have considerable literature precedent,[53−55] but the internal nature of the E^{2-} ligands in the present system, coupled with the difference in formal oxidation state, gives a structure with compositionally ordered S^{2-} and $(Se_2)^{2-}$ ligands for the chemically distinct sites and no evidence to suggest the presence of Se^{2-} or $(SSe)^{2-}$.

The optical properties also reflect the structural arguments indicating Er is bonded in an environment where S, Se, and I are its nearest neighbors. The reported 3 ms emission lifetime is typical of a low phonon energy host, which is supported by Table 3 where the emission lifetimes of various classes of low phonon energy hosts are summarized and found to range from 2.3 to 30 ms. More specifically, Er ions encapsulated by selenide, sufide, or iodide have lifetimes that range from 2.3 to 4 ms.[26−8] In contrast, molecular complexes of Er typically exhibit lifetime data in the microsecond range,[31−6] which are characteristic of high phonon energy materials.

In Er^{3+} compounds one of the principle channels of multiphonon nonradiative decay is via $^4I_{11/2} \rightarrow {}^4I_{13/2}$, which is in the frequency region of 3700 cm^{-1}. This nonradiative channel can reduce the effective population density at $^4I_{13/2}$ and hence the fluorescence decay time and efficiency of the 1540 nm emission. Similarly the population of the $^4I_{13/2}$ state during the $^4I_{13/2} \rightarrow {}^4I_{15/2}$ decay can be further lost by vibrational groups of frequency 6500 cm^{-1}. If Er^{3+} is directly attached to any of these vibrational groups or its harmonics, higher nonradiative loss can be expected with low quantum efficiency as observed in all molecular Er complexes reported to date. In most of the molecular complexes the two main vibrational groups quenching the fluorescence efficiency of Er^{3+} are C−H and O−H. The second-order vibrational energy of C−H (2960 cm^{-1}) is resonant with the Er^{3+} first excited state (6500 cm^{-1}). Similarly O−H is one of the potential quenchers of Er luminescence, because its first vibrational overtone (3400 cm^{-1}) is strongly resonant with the $^4I_{13/2} \rightarrow {}^4I_{15/2}$ transition (6500 cm^{-1}). Cluster **2** has a complete absence of C−H or O−H vibrational groups in the core, and the CH groups from the THF ligands are distantly connected to Er through a relatively weak dative bond.

Table 3. Comparison of the Fluorescence Lifetime and Phonon Frequencies of Some Reported Er-Containing Solid-State Materials

host	lifetime (ms)	phonon frequency (cm^{-1})	reference
sulfide	3.0	450−700	28
selenide	2.3	450−700	27
tellurite	4	450−700	26
germanate	6	900	26
ZBLA fluoride glass	10	500	26
fluorides, chlorides	10−30	200−400	26
yttrium aluminum garnet	8	400	26

The low phonon nature of **2** also explains why the estimated quantum efficiency value of 78% is so high, in fact the highest value reported for a molecular compound containing Er. When comparing the fluorescence spectral width (fwhm) and stimulated emission cross section to those of other low phonon energy hosts such as LaF_3/Er,[42] similar values are obtained (Table 2). The radiative quantum efficiency of Er^{3+} in LaF_3 nanocrystals is estimated to be 100% with a spectral bandwidth of 73 nm and a stimulated emission cross section of 3.3×10^{-21} cm^2, almost identical to the values of 61 nm (fwhm) and 4.1×10^{-21} cm^2 for **2**.

Conclusion

Lanthanide clusters with internally coordinated Ln ions are synthetically possible, provided that a balance is struck between solvent and chalcogenido basicity. Key to this approach is the use of less basic chalcogens to chemically "cap" more basic LnE cores. These chalcogen rich materials have absorption and emission properties comparable to those of Er-doped solid-state materials and, as soluble compounds, are potentially useful for delivering emissive Er ions into organic polymers.

Acknowledgment. This work was supported by the National Science Foundation under Grant No. CHE-0303075.

Supporting Information Available: X-ray crystallographic files in CIF format for the crystal structures of **1** and **2**. This material is available free of charge via the Internet at http://pubs.acs.org.

JA043655Z

(47) Iandelli, A. *Z. Anorg. Allg. Chem.* **1956**, *288*, 81−6.
(48) Guittard, M.; Benacerraf, A. *Compt. Rend.* **1959**, *248*, 2589−91.
(49) Beck, G.; Nowacki, W. *Naturwissenschaften* **1938**, *26*, 495−6.
(50) Haase, D. J.; Steinfink, H.; Weiss, E. J. *Inorg. Chem.* **1965**, *4*, 538−40.
(51) Haneveld, A. J. K.; Jellinek, F. *J. Less-Common Met.* **1971**, *24*, 229−31.
(52) Podberezskaya, N. V.; Pervukhina, N. V.; Belaya, S. V.; Vasilieva, I. G.; Borisov, S. V. *J. Struct. Chem.* **2001**, *42*, 617−627.
(53) Mori, H.; Suzuki, H.; Okano, T.; Moriyama, H.; Nishio, Y.; Kajita, K.; Kodani, M.; Takimiya, K.; Otsubo, T. *J. Solid State Chem.* **2002**, *168*, 626.
(54) Dehnen, S.; Zimmermann, C.; Anson, C. E. *Z. Anorg. Allg. Chem.* **2002**, *628*, 279.
(55) Sekar, P.; Ibers, J. A. *Inorg. Chim. Acta* **2001**, *319*, 117.